Photothermal laser speckle imaging

Caitlin Regan,[1,2] Julio C. Ramirez-San-Juan,[3] and Bernard Choi[1,2,*]

[1]*Department of Biomedical Engineering, University of California, Irvine, 3120 Natural Sciences II, Irvine, California 92697, USA*

[2]*Beckman Laser Institute and Medical Clinic, University of California, Irvine, 1002 Health Sciences Road East, Irvine, California 92612, USA*

[3]*Optics Department, INAOE, Luis Enrique Erro No. 1, Tonantzinla, Puebla 72840, Mexico*

**Corresponding author: choib@uci.edu*

Received March 31, 2014; revised June 9, 2014; accepted July 7, 2014;
posted July 25, 2014 (Doc. ID 209069); published August 18, 2014

The analysis of speckle contrast in a time-integrated speckle pattern enables visualization of superficial blood flow in exposed vasculature, a method we call laser speckle imaging (LSI). With current methods, LSI does not enable visualization of subsurface or small vasculature, because of optical scattering by stationary structures. In this work we propose a new technique called photothermal LSI to improve the visualization of blood vessels. A 595 nm laser pulse was used to excite blood in both *in vitro* and *in vivo* samples. The high absorption coefficient of blood at this wavelength results in efficient conversion of optical energy to thermal energy, resulting in an increase in the local temperature and hence increased scatterer motion, and thus a transient decrease in speckle contrast. As a result, we found that photothermal LSI was able to visualize blood vessels that were hidden when imaged with a conventional LSI system.

OCIS codes: (110.0113) Imaging through turbid media; (110.6150) Speckle imaging; (350.5340) Photothermal effects.
http://dx.doi.org/10.1364/OL.39.005006

In 1981, Fercher and Briers [1] first proposed the use of time-integrated laser speckle patterns to map blood flow in the retina. Dunn *et al.* [2] demonstrated that this method enabled blood-flow mapping of the rodent brain, which led to a rapid increase in the use of laser speckle imaging (LSI) for a wide variety of biological and biomedical applications.

Typically, researchers use LSI to map and quantify relative changes in blood flow in response to an intervention. A related use of LSI is simply to enable visualization of perfused microvasculature [3]. However, scattering layers such as the skull or epidermis obscure the microvascular architecture. A variety of postprocessing methods were proposed to reduce this effect, including temporal processing [4] and motion contrast algorithms [5].

Here we propose a new method, which we call photothermal LSI, to noninvasively image subsurface blood vessels using selective optical excitation of absorbers within the vessels. Photothermal LSI is based on two techniques described previously in the literature: magnetomotive LSI [6] and pulsed photothermal radiometry (PPTR) [7,8]. Magnetomotive LSI involves the use of an alternating magnetic field to induce movement of superparamagnetic iron oxide nanoparticles that are introduced into the vasculature. The additional motion of the particles aligning back and forth with the alternating magnetic field causes a distinct increase in motion that the LSI method detects as a decrease in local speckle contrast.

PPTR involves application of a short pulse of laser light to the surface of a sample, resulting in selective absorption and subsequent heating of specific optical absorbers within the medium. Mid-infrared detectors are typically used to collect infrared emission at the sample surface that varies because of heat diffusion from the heated absorbers. Based on analysis of the transient change in infrared emission, specific parameters can be estimated, including tissue absorption coefficients [8] and depth of vasculature [7].

Photothermal LSI involves use of a short pulse of laser light (similar to PPTR) to heat subsurface blood vessels, which we propose leads to a transient decrease in speckle contrast because of photothermally-induced changes to intravascular optical scatterers. This is similar to magnetomotive LSI; however, we selectively target absorption by the hemoglobin molecules contained within the red blood cells, rather than modulate the movement of an exogenous particle. To achieve selective optical excitation, we induce transient heating of the blood with a 595 nm laser pulse. In this Letter, we present data collected with *in vitro* and *in vivo* experimental setups, to demonstrate the ability of photothermal LSI to improve visualization of subsurface microvasculature via a targeted increase in the difference in contrast between the blood vessels and surrounding tissue.

For our *in vitro* experiments, we used two samples: a 1 cm wide cuvette filled with porcine blood [Fig. 1(a)], to demonstrate the concept, and a microchannel-based skin phantom [Fig. 2(a)]. To create the phantom, a slide with microchannels (thinXXS Microtechnology AG, Germany) was placed above a silicone block containing TiO_2 powder to mimic the scattering properties of soft biological tissues. A second silicone layer (400 μm thick), with TiO_2

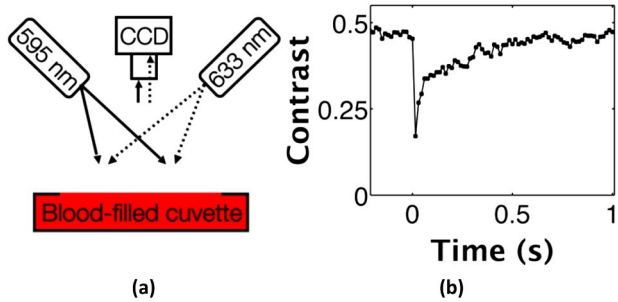

Fig. 1. *In vitro* photothermal LSI of blood in a cuvette. (a) Photothermal LSI setup with 633 nm imaging laser light and 595 nm pulsed dye laser to excite the blood. Images are captured with a cooled CCD camera with a laser-line bandpass filter to block extraneous light. (b) Speckle contrast versus time plot illustrates distinct drop in contrast corresponding to the photothermal excitation pulse at time 0 s. The 60% decrease in contrast returns to baseline over about 0.6 s as the blood returns to room temperature.

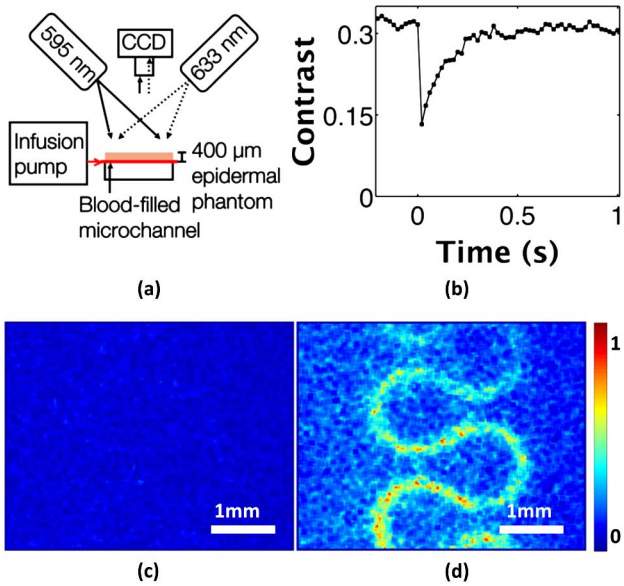

Fig. 2. *In vitro* photothermal LSI of blood flowing through a microchannel. (a) Photothermal LSI setup with blood infused into the system at 4 mm/s and a 400 μm epidermal phantom placed above the microchannel. (b) Speckle contrast versus time in a region of interest above the channel shows a 60% decrease in flow occurring after the excitation pulse at time 0 s, and returning to baseline over the next ~0.4 s. (c) Normalized speckle flow index (SFI) in microchannel before the photothermal excitation (Media 1). (d) SFI image after the excitation pulse (Media 1) shows the blood flow in the channel clearly visible beneath the skin-simulating phantom.

powder to simulate epidermal scattering properties, was placed above the microchannel. An infusion pump was used to inject porcine blood (Sierra for Medical Science, Whittier, CA) into the microchannel, which had an inner diameter of 320 μm. Tygon tubing was used to deliver the blood from the syringe pump to the channel inlet. The infusion pump was set to achieve a flow speed of 4 mm/s, representative of flow in arterioles and venules [9].

To image the dynamics of particle motion, we used a conventional LSI system consisting of a 632.8 nm HeNe laser that uniformly illuminated either the blood-filled cuvette or the skin phantom [Figs. 1(a) and 2(a)]. The radiant exposure of this imaging laser is ~11 mJ/s, or less than 0.0001% of the radiant exposure of the interrogating pulse, making its contribution to any photothermal changes in the sample negligible. All speckle images were acquired with a HotShot 1280 CCD camera (NAC Image Technology, Simi Valley, CA, USA) equipped with a macro lens. To mitigate specular reflectance from the samples, a polarizing filter was placed in front of the camera lens and perpendicularly oriented to the polarization of the incident light.

We used pulsed 595 nm laser light (Vbeam, Candela, MA) to optically excite the samples. We selected 595 nm because of the strong absorption of this wavelength by hemoglobin. For our experiments, we used a pulse duration of 3 ms and radiant exposure of 4 J/cm^2, which is similar to radiant exposures used previously in PPTR studies [7]. We used a laser-linepass filter (ThorLabs, Newton, NJ) centered at 632.8 nm (70% transmission) to prevent contamination of images by remitted 595 nm laser light (less than 0.01% transmission).

We collected raw speckle images at 50 frames per second with an exposure time of 14 ms, before, during, and after application of the pump 595 nm light. We used the standard sliding-window algorithm (7×7 pixel dimension) to convert each raw speckle image to a speckle contrast image [10]. From each speckle contrast image, we calculated the mean speckle contrast within a 16×66 pixel region of interest. We then calculated maps of speckle flow index (SFI) using a simplified speckle imaging equation [10].

Upon photothermal excitation of a blood-filled cuvette, [Fig. 1(a)], we observed a transient reduction of speckle contrast [Fig. 1(b)]. The contrast decreased abruptly by ~60%, suggesting an increase in motion of scattering particles within the blood. After ~0.6 s, the contrast returned nearly to its baseline value, presumably because of a decrease in temperature of the excited sample.

Similarly, with photothermal excitation of the microchannel-based skin phantom [Fig. 2(a)], we observed a transient reduction in speckle contrast [Fig. 2(b)]. To simulate subsurface blood flow, we placed a skin-simulating phantom of 400 μm thickness on top of the microchannel. In this specific case, to mimic *in vivo* conditions, the blood continuously flowed through the microchannel; therefore, the associated speckle contrast values at all time points were lower than those for the blood-filled cuvette. We observed a ~60% decrease in the contrast following photothermal excitation, and a return to baseline contrast after ~0.4 s. Prior to photothermal excitation, it was not possible to visualize the microchannel through the overlying epidermal phantom [Fig. 2(c)]. Immediately after photothermal excitation, the microchannel structure was clearly evident [Fig. 2(d)]. We postulate that this is because of an increase in the temperature of the blood, creating more movement of scattering particles present in the blood in the microchannel. Media 1 [Figs. 2(c) and 2(d)] shows a video clip of SFI dynamics during photothermal excitation of the microchannel. In summary, the data shown in Fig. 2 collectively supports the hypothesis that photothermal excitation of flowing blood in an *in vitro* system induces a brief decrease in speckle contrast that is observed even when the flowing blood is below a surface layer.

We next investigated how photothermal LSI performs with an *in vivo* animal model. To enable direct comparison of the imaged microvasculature with the actual microvascular architecture, we used a mouse dorsal window chamber model [11] as our test substrate [Fig. 3(a)]. Briefly, the window chamber is a surgical preparation in which one full thickness of skin is suspended between titanium frames. A microvascular network is readily visible from the subdermal side of the chamber; the epidermis of the intact skin thickness is visible on the other side.

For LSI, we achieved wide-field coherent illumination of the epidermal side of the window chamber with the use of an 808 nm laser diode (Ondax, Monrovia, California, USA) and an engineered diffuser. To achieve photothermal excitation, we used the same pulsed-dye laser settings as in the *in vitro* experiments. We collected raw speckle images at 100 fps with a 9 ms exposure time. We used a longpass optical filter (ThorLabs, Newton, NJ) with an 800 nm wavelength cutoff to block stray light

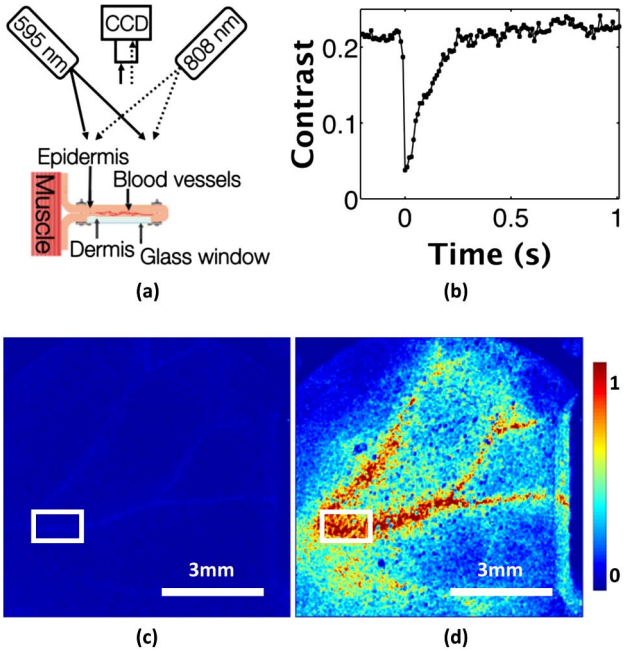

Fig. 3. *In vivo* photothermal LSI in a mouse dorsal window chamber model. (a) Imaging setup of the epi-illuminated reverse side of the window chamber. An 808 nm laser light is used to illuminate the epidermis for imaging, and an 800 nm longpass filter is placed on the CCD camera to block stray 595 nm excitation light. (b) Speckle contrast versus time in the region of interest highlighted in (c) and (d). The contrast drops by 80% when the excitation pulse is fired at time 0 s, and quickly returns to baseline over ~0.3 s. (c) Normalized SFI image before the excitation pulse (Media 2). (d) SFI image after the photothermal excitation (Media 2) shows increased motion in the vessels. The perivascular increase in the SFI is probably because of smaller vessels and capillaries that cannot be resolved with our current imaging system.

associated with the excitation pulse. The filter allows for 85% transmission of 808 nm light, and completely blocks 595 nm light (~10^{-6}% transmission). We computed speckle contrast images using the spatial speckle-imaging algorithm with a 7×7 structuring element. From each contrast image, we selected a 16×66 pixel region of interest within one of the larger vessels [denoted by the rectangular region in Figs. 3(c) and 3(d)].

Following the photothermal excitation, the speckle contrast decreased by ~80% [Fig. 3(b)]. After ~0.3 s, the speckle contrast in the region of interest returned to its baseline value, presumably because of a mix of heat diffusion from the irradiated site and advection via blood flow. From direct inspection of the SFI maps, the increase in visualization of the vasculature is apparent [Media 2, Figs. 3(c) and 3(d)]. In a direct comparison of the SFI images from the *in vitro* [Fig. 2(d)] and *in vivo* [Fig. 3(d)] images, we observed *in vivo* a larger perivascular increase in SFI that is more diffuse in appearance. We hypothesize that this increase is because of a similar photothermal effect in blood vessels that are too small to resolve with the current experimental setup. This resolution issue can be overcome with a proper choice of higher-magnification camera optics.

Photothermal LSI relies on the concept of pulsed excitation of targeted absorbers, in our case red blood cells, to enhance the contrast of vasculature below a static scattering layer. The exact mechanism for this change in contrast is currently unknown. Using the equation $\Delta T = H\mu_a/\rho c$ [12] where H is the radiant exposure (4 J/cm^2), μ_a is the absorption coefficient of blood at 595 nm (36 cm^{-1}) [13], ρ is the density of whole blood (1050 kg/m^3) [14], and c is the mass specific heat capacity (3617 J/kg/K) [14], we calculated the estimated peak rise in temperature of the blood because of absorption at 595 nm to be ~38°C, assuming there is no convective or diffusive losses during the pulse. Depending on the tissue geometry of interest, we anticipate that lower radiant exposures and hence peak temperature rises may be sufficient to improve visualization of subsurface blood vessels.

We hypothesize that the increase in the SFI is associated with a rapid diffusion of generated heat from the hemoglobin in red blood cells to nearby plasma proteins. We speculate that the change in motion because of this change in temperature may be caused by thermal expansion, changes in viscosity, or increases in diffusive motion, but further research will be needed to determine the mechanism. We also observe a similar transient change in speckle contrast when photothermal LSI is applied to a solution of India Ink and Intralipid (data not shown), demonstrating that this phenomenon is not only associated with whole blood.

In conclusion, a photothermal LSI involves a transient, nondestructive increase in temperature in the vasculature, resulting in a decrease in speckle contrast and hence an increase in the SFI. We propose that this method may enable improved three-dimensional localization of sources of speckle contrast; with accurate knowledge of the microvascular structure and local optical properties, researchers can use advanced tomography methods [15] to better define the speckle correlation time associated with subsurface blood vessels.

This research was funded in part by CONACYT (CB-2010-156876-F), the Arnold and Mabel Beckman Foundation, the Air Force Office of Scientific Research (FA9550-14-1-0034), the National Institute of Health (R01 DE022831, R01 HD065536), the National Institute of Health Laser Microbeam and Medical Program (P41 EB015890), and the NSF BEST IGERT program (DGE-1144901). The authors would also like to thank Chelsea Pittman (UC-Irvine) for performing the animal surgeries, and Andrew Weatherbee (University of Toronto), Dr. Boris Majaron (Institut Jožef Stefan, Slovenia), and Dr. Enrico Gratton (UC-Irvine) for insightful discussions into potential mechanisms related to the photothermal LSI.

References

1. A. F. Fercher and J. D. Briers, Opt. Commun. **37**, 326 (1981).
2. A. K. Dunn, T. Bolay, M. A. Moskowitz, and D. A. Boas, J. Cereb. Bl. F. Metab. **21**, 195 (2001).
3. J. J. Qiu, P. C. Li, W. H. Luo, J. Wang, H. Y. Zhang, and Q. M. Luo, J. Biomed. Opt. **15**, 016003 (2010).
4. P. C. Li, S. L. Ni, L. Zhang, S. Q. Zeng, and Q. M. Luo, Opt. Lett. **31**, 1824 (2006).
5. R. Liu, J. Qin, and R. K. K. Wang, J. Biomed. Opt. **18**, 060508 (2013).

6. J. Kim, J. Oh, and B. Choi, J. Biomed. Opt. **15**, 011110 (2010).
7. B. C. Li, B. Majaron, J. A. Viator, T. E. Milner, Z. P. Chen, Y. H. Zhao, H. W. Ren, and J. S. Nelson, J. Biomed. Opt. **9**, 961 (2004).
8. S. A. Prahl, I. A. Vitkin, U. Burggemann, B. C. Wilson, and R. R. Anderson, Phys. Med. Biol. **37**, 1203 (1992).
9. V. S. Kalambur, H. Mahaseth, J. C. Bischof, M. C. Kiebik, T. E. Welch, A. Vilback, D. J. Swanlund, R. P. Hebbel, J. D. Belcher, and G. M. Vercellotti, Am. J. Hematol. **77**, 117 (2004).
10. O. Yang, D. Cuccia, and B. Choi, J. Biomed. Opt. **16**, 016009 (2011).
11. A. J. Moy, S. M. White, E. S. Indrawan, J. Lotfi, M. J. Nudelman, S. J. Costantini, N. Agarwal, W. Jia, K. M. Kelly, B. S. Sorg, and B. Choi, Microvasc. Res. **82**, 199 (2011).
12. B. Choi and A. J. Welch, Lasers Surg. Med. **29**, 351 (2001).
13. S. A. Prahl, "Tabulated molar extinction coefficient for hemoglobin in water," March 4, 1998. http://omlc.ogi.edu/spectra/hemoglobin/summary.html.
14. P. A. Hasgall, E. Neufeld, M. C. Gosselin, A. Klingenbock, and N. Kuster, "IT'IS Database for thermal and electromagnetic parameters of biological tissues," Version 2.4, July 30, 2013, www.itis.ethz.ch/database.
15. T. B. Rice, E. Kwan, C. K. Hayakawa, A. J. Durkin, B. Choi, and B. J. Tromberg, Biomed. Opt. Express **4**, 2880 (2013).